American Mineralogist, Volume 60, pages 1063–1068, 1975

Nontronite Topotaxial after Hedenbergite

RICHARD A. EGGLETON

Department of Geology, Australian National University, Canberra, Australia

Abstract

Hedenbergitic pyroxene alters topotaxially to the smectite nontronite following loss of Ca, Mg, and some Si, oxidation of the ferrous iron, and hydration. One unit cell of nontronite forms pseudomorphically from 1½ unit cells of pyroxene with no volume change; the *b* axes in nontronite and pyroxene are parallel but c_{pyx} equals a_{nont} so that d_{100} for pyroxene becomes d_{001} for nontronite. The nucleation of nontronite proceeds from cracks, but first-formed domains, which are about 50 × 10 × 3 nm, are distributed homogeneously over small (micron) areas within the pyroxene. It is postulated that these domains form by a process similar to crystallographic shear. Silicon-ferric iron, tetrahedral-octahedral chains slip $\frac{1}{2}[10\bar{1}]_{pyx}$ to reconnect as 'talc' layers after loss of Ca, Mg, Si, and O has left room for movement. The resulting clear, yellow, nontronite crystals are one-dimensionally disordered, and have composition $(K_{0.06}Ca_{0.24})\ (Al_{0.05}Fe^{3+}_{3.40}Mg_{0.55})Si_8O_{20}(O,OH)_4 \cdot 4.3\ H_2O$.

Introduction

In 1970, realignment of the Barton Highway 12 km north of Canberra, A.C.T., exposed a pocket of apple-green clay about 1m × 2m in a road cutting. Samples were collected from the cutting, and a preliminary study of the outcrop was made by Mr. S. Ozimic of the Bureau of Mineral Resources. The clay pocket lies on a narrow skarn at least 2 km long, is marked at the surface by quartz and goethite, and has pyroxene, actinolite, and epidote as major primary minerals. This outcrop has probably formed from the Silurian Canberra Group calcareous sandstone.

Pyroxene

The most abundant mineral in the skarn is the pyroxene hedenbergite; its composition and physical properties are given in Table 1. In most hand specimens of the skarn the pyroxene grains are equidimensional, about 0.01–0.1 mm across, and show good {100} parting. Irregular patches of larger crystals, or of pseudomorphs of clay and goethite after hedenbergite, are prominent in the face of the cutting. These crystals are bladed and radiating, with {100} well developed, and reach several centimeters in length. Most of the larger crystals are multiple-twinned on {100}, although more than ten individuals in a crystal are uncommon. The twin surface is a major locus of alteration of the hedenbergite.

Nontronite

Single crystals of nontronite occur on the (100) parting surface of the pyroxene. Their occurrence and morphology might suggest that they are pseudomorphs after hedenbergite; however, careful study of the nontronite, and of the process of formation of the nontronite from hedenbergite, shows that the nontronite has formed by topotaxial alteration of the hedenbergite. That is, the detailed atomic structure of the pyroxene is inherited by the nontronite, not just its outer form. Because the nontronite has formed from pyroxene, because the crystals are small, and because partly-altered pyroxene and fully-altered pyroxene (*i.e.*, nontronite) are visibly indistinguishable, it is not possible to collect large quantities (say 0.1 g) of nontronite and be sure that no submicroscopic pyroxene is included. Despite this difficulty, this section describes the nontronite as it is; in the next section the alteration process is described, and the intimate relation between the two minerals documented.

The nontronite crystals are pale yellow, with perfect {001} cleavage and hardness less than 1, deduced from the observation that they are more vulnerable to damage by touch than are talc crystals of comparable quality. A few exceptional crystals have grown in vugs, and show prismatic faces (Fig. 2a). The prismatic faces give poor light reflection; however, both the average of 8 measurements and

TABLE 1. Analyses of Pyroxene and Nontronite

	Pyroxene			Nontronite		
	A	B	C	D	E	F
SiO_2	50.56	49.98	52.83	55.67		53.12
Al_2O_3	0.26	N.D.	0.38	N.D.		0.36
Fe_2O_3	*	*	32.79	31.12		29.69
FeO	17.32	22.14		*	2.33	*
MnO	0.17	N.D.	0.03	N.D.		0.03
MgO	8.29	4.78	3.33	2.61		2.49
CaO	22.63	22.82	3.76	1.58		1.51
K_2O	0.06	N.D.	0.31	N.D.		0.30
H_2O	N.D.	N.D.	N.D.	N.D.	12.5	12.50
Σ	99.3	99.7	93.43	90.80		'100.00'
Si	8.0	8.0				8.0
Al	0.0	*				0.05
Fe^3	*	*				3.40
Fe^2	2.3	3.0				*
Mg	1.9	1.1				0.55
Ca	3.8	3.8				0.24
K						0.06
a_{pyx}/d_{001} nont	0.987 nm			1.42 nm		
b	0.901			0.910		
c or a	0.526			0.525		
β	105.3°			-		
D	-			2.2		
α	-			1.54		
β	-			1.583		
γ	-			1.585		
2Vα meas	122°			20°-26°		
2V calc	-			24°		
γ ∧ c	49°			0°		

N.D. - not determined
* - not determined, assumed zero.

(A, B: *pyroxene, structural formula to 24 oxygens.* C, D, E: *nontronite.* F: *analysis* D *corrected for water loss during electron beam heating. Structural formula from cell volume and density.)*

the clearest single measurement give an intercleavage angle of 76°. From X-ray measurements, (012)∧(012) calculates at 75.9° for nontronite. These crystals resemble pyroxene laths showing {100} and {110}; however, a reduction of the pyroxene cleavage angle from 93° to 76° requires a relative change in dimension of 30 percent. As will be described below, there is no textural evidence whatsoever for a dimensional change during the formation of nontronite from pyroxene, and it is concluded that the nontronite crystals indeed show the form {012}.

X-ray diffraction study of single crystals and powdered crystals shows that the basal spacing of 1.42 nm expands to 1.7 nm after soaking in ethylene glycol, and collapses to 1.0 nm on heating above 300°C. The collapse on heating becomes irreversible above 350°C. All single crystal reflections of the nontronite are streaked parallel to c^*, indicating stacking disorder. The *hk* section of the reciprocal lattice has plane group symmetry *cmm*, and it is concluded from this symmetry that the disorder is translational only. The nontronite layer has symmetry *C2/m*.

Transmission electron-micrographs show that small domains (*ca* 50 × 10 × 3 nm) of pyroxene are present in much optically homogeneous nontronite, so that bulk physical and chemical results are unlikely to refer to pure nontronite. Analysis D (Table 1) is the average of 12 analyses made on reflective cleavage surfaces of six grains, one of which was later crushed, and examined by transmission electron-microscopy. No pyroxene was detected by selected area diffraction, but some flakes showed the domains referred to above. Analysis C (Table 1) is of nontronite in polished thin-section formed from the pyroxene listed as analysis A of Table 1. Both the Ca content and $2V$ of this nontronite suggest it has relict pyroxene domains.

The refractive index γ is low for nontronite (1.58 compared with 1.64 for nontronite containing 32 percent Fe_2O_3 (Ross and Hendricks, 1945)). The index α, calculated from birefringence calibrated from adjacent pyroxene, is likewise low. Index of refraction measurements of smectites are difficult to make because of penetration of the clay by the immersion oil. The crystals used in this study absorbed glycol very slowly, and it is concluded that they would absorb immersion oil more slowly than would the finer grained samples recorded by Ross and Hendricks. The indices reported here represent the material studied, not the same material saturated with immersion oil, and so do not compare with previously published values. Density was measured in a density gradient with a range from 1.9 to 2.4, measurable to 0.003.

The structural formula (Table 1, F) is derived largely from analysis D, 'corrected' to total 100 percent by inclusion of 12.5 percent water as measured on sample E, and the Al_2O_3 and K_2O percentages from sample C. In adopting this procedure, it is assumed that some water was volatilized by the electron-probe beam. The corrected analysis was calculated to the cell content using the measured density and cell volume. Despite the very approximate 'correction' to analysis D, the structural formula is remarkably close to an ideal smectite formula in which the charge deficiency arises in the octahedral sheet. The crystals have composition $(Ca,K)_{0.3}(Al, Fe^{3+},Mg)_4Si_8O_{20}(O,OH)_4 4.3H_2O$.

Alteration

Optical and X-ray Observations

Along fractures, the hedenbergite is altered to a fine-grained random aggregate of yellow nontronite. Similar alteration occurs along cleavage cracks, par-

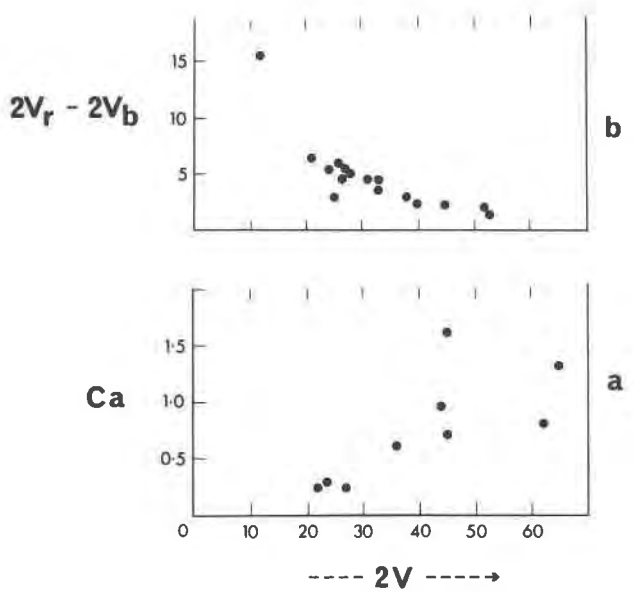

FIG. 1. Variation of properties with alteration from pyroxene to nontronite. a. Ca (per 8 Si) *vs* $2V\alpha$; b. optic axial dispersion (universal stage measurements).

ticularly at the ends of the hedenbergite crystals. In marked contrast, nontronite development along the {100} parting occurs in crystallographic continuity with the hedenbergite. During this process, the 0.9 nm *b* axes of both phases remains common, as does the 0.52 nm axis (pyroxene *c* = nontronite *a*). The course of the alteration is shown by an increase in the depth of the yellow color of the forming crystals, by a change in $2V_\gamma$ from 62° in hedenbergite to 160° (biaxial negative) in nontronite, and by an increase in optic axial dispersion (Fig. 1).

The first developed discrete yellow flakes have a $2V\alpha$ of about 60°, are soft, inelastic, and striated parallel to the pyroxene *c* axis. Their X-ray reflections are fairly sharp pyroxene reflections, except that the row a^* cannot be detected, and diffuse streaks occur parallel to a^* in other rows. A broad peak is present at 1.6 nm corresponding to d_{001} for nontronite. Its integral peak width of about 2° 2θ (Co$K\alpha$) suggests that the nontronite domains are about 5 nm thick (Guinier, 1963).

As $2V\alpha$ decreases further, the pyroxene reflections weaken and the diffuse streaks increase in intensity. At $2V\alpha \sim 20°$, the yellow nontronite crystals have lost the striations visible in crystals of higher $2V$ and appear optically homogeneous. Their reciprocal lattice is in the form of continuous rods along the original pyroxene rows parallel to a^*.

Chemistry

All chemical analyses were done using the Cambridge Geoscan Electron Microprobe at the Geology Department of the University, Manchester (F.C.F. Wilkinson, analyst). Very poor polish on altered pyroxene makes these analyses inaccurate, but one such analysis is reported (analysis C), as it represents alteration of the pyroxene of analysis A. Good nontronite crystals such as were used in analysis D are far too rare to allow determination of FeO or H_2O. Scrapings from clean skarn surfaces, however, produced 150 mg of fairly pure nontronite with $2V$ between 40° and 60° from which FeO and H_2O were determined. The totals for the nontronite analyses indicate considerable volatilization of water by the electron beam.

Transmission Electron Microscopy

The alteration process from pyroxene to nontronite was examined by transmission electron-microscopy, and electron diffraction, on cleavage

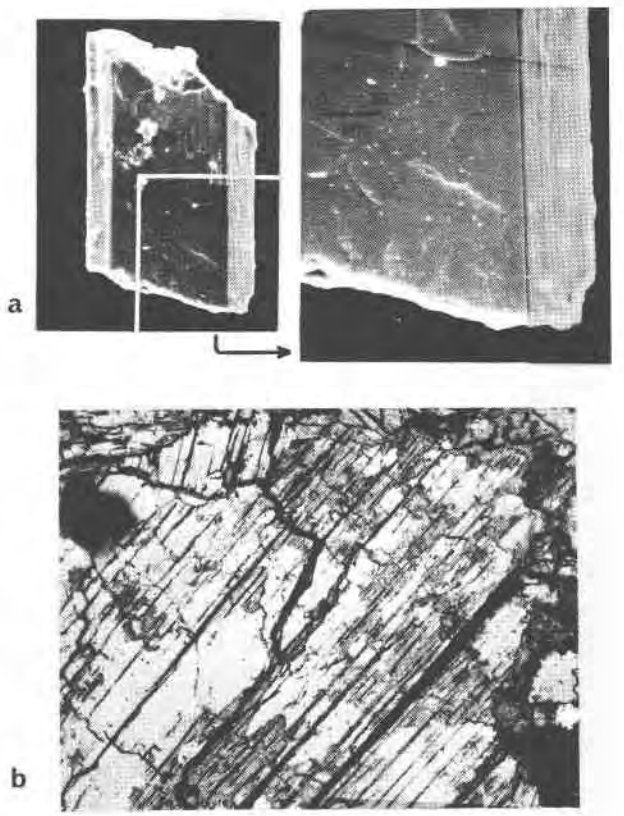

FIG. 2. a. SEM micrograph of a single nontronite crystal; b. optical micrograph (reflected) of nontronite (gray) in pyroxene (whiter), demonstrating constant volume alteration.

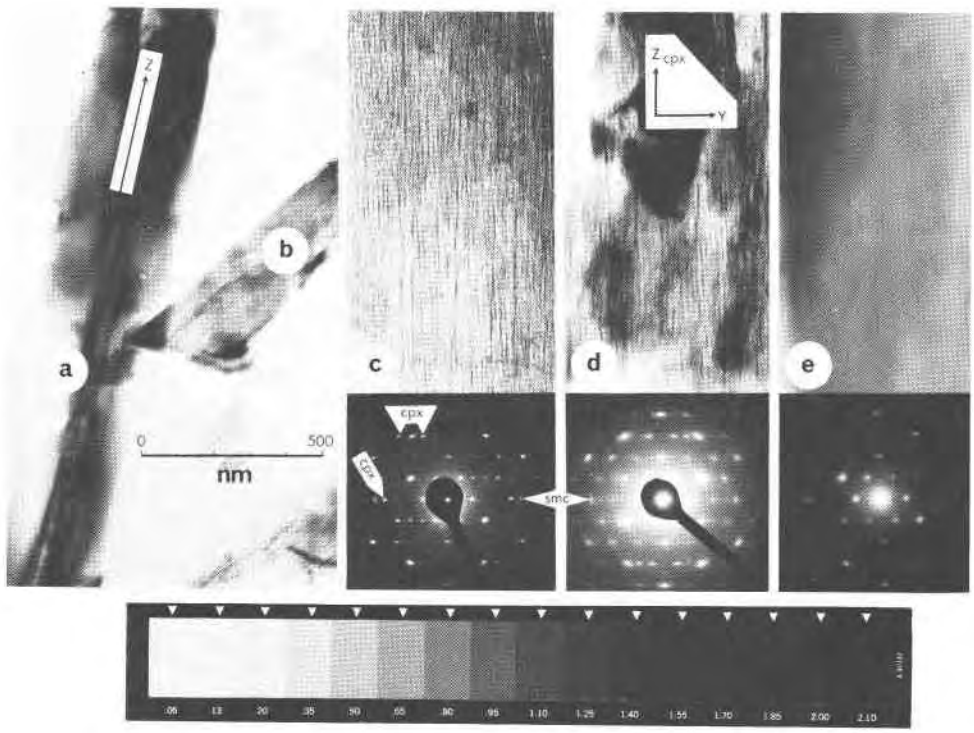

FIG. 3. TEM micrographs of successive stages of alteration, all grains lying on cleavage. cpx – pyroxene reflections, smc – nontronite. a. fresh pyroxene; b. initial alteration; c. estimated to be ½ altered, pyroxene reflections still prominent; d. about 75 percent altered—sample $2V$ between 40° and 50°; e. crushed nontronite crystal, $2V = 23°$, no pyroxene reflections visible.

fragments and on ion-thinned samples using an AEI EM6G electron microscope operating at 100 kV. Figure 3 shows a series of crushed flakes, ranging from unaltered pyroxene (3a) to nontronite (3e). Electron diffraction patterns from partly altered material (Fig. 3b, c, d) show both pyroxene and nontronite diffraction spots. The dark stripes visible in the micrographs are parallel to the pyroxene chain axis, *c*; dark field microscopy confirms that the stripes are alternately pyroxene and nontronite. Figure 4 shows an interpretation of Figure 3 based on measurements of the micrographs. At the start of alteration narrow nontronite domains form in the pyroxene (Fig. 4a). With increased alteration the nontronite domains widen and new ones form (Fig. 4b, c) until the whole crystal is made over to nontronite. At $2V = 25°$, cleavage flakes are essentially featureless, and selected area diffraction patterns show nontronite reflections only (Fig. 3e).

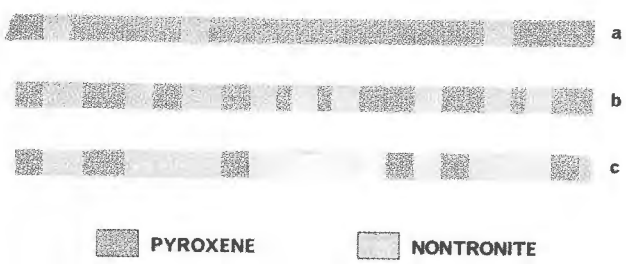

FIG. 4. Interpretation of the stripes in Figure 3. Dark stripes: pyroxene; light stripes: nontronite. The narrowest stripe is approximately 1.8 nm wide, corresponding to $2 \times b$ for either structure. a. formation of few nontronite domains (*cf* Fig. 3b); b. enlargement of nontronite domains and formation of new ones, 50 percent alteration (*cf* Fig. 3c); c. further enlargement of nontronite domains to about 75 percent alteration (*cf* Fig. 3d).

Although it is clear from thin-section examination that alteration is localized at fractures in the pyroxene, there is no evidence in the electron micrographs that nontronite nucleates at such a fracture or at grain (twin) boundaries. The nontronite domains are distributed uniformly over any one flake or section, varying only in quantity from flake to flake, thus nucleation of nontronite in pyroxene is homogeneous.

Volume Changes

In order to calculate the element balance between the pyroxene and its alteration, a careful search was

made for evidence of volume change during alteration. Optical study shows no warping or distortion, or expansion or contraction (Fig. 2b). Scanning electron microscopy reveals minor splitting of some nontronite crystals along {001} but no distortion of individual crystals, even where optical evidence exists of patchy alteration. Transmission electron microscopy shows no dislocations, nor any other evidence of strain at boundaries between nontronite and pyroxene domains (Fig. 3). It is concluded that the alteration from pyroxene to nontronite takes place at constant volume.

Chemical changes during pyroxene alteration calculated at constant volume amount to the loss of 95% Ca, 75% Mg, and 30% Si, Fe remaining constant. During this process the ferrous iron is oxidized and 1.4 percent hydrogen added. The 2.33 percent FeO in analysis E is interpreted as residual hedenbergite.

Mechanism

Coherence between the lattices of hedenbergite and nontronite is evident from their parallel optics, equal and parallel lattice edges as determined by X-ray diffraction and electron diffraction, and the absence of dislocations at domain boundaries (Fig. 3). The crystallographic coherence, coupled with the morphological evidence for constant volume alteration, strongly suggests that the alteration proceeds with minimal disruption of the pyroxene structure. The first nontronite domains are elongate parallel to the pyroxene tetrahedral chain direction; it is in this direction that fewest bonds are broken.

In pyroxene the tetrahedral chains and the *M*1 octahedra sandwiched between them form structural units that resemble the talc sheet of a layer silicate. It is suggested that these structural units retain their identity during the alteration, in which protons attach to the lateral oxygens of the tetrahedral chains, thereby releasing Ca^{2+} with simultaneous oxidation of Fe^{2+} to Fe^{3+}.

$$Ca_2Fe_2^{2+}Si_4O_{12} + 2H^+ \rightarrow Fe_2^{3+}Si_4O_{10}(OH)_2 + 2Ca^{2+}$$

Although this simple process produces almost exactly the nontronite's talc sheet composition, it does not explain the interlayer water, and because the alteration proceeds at constant volume, extra water cannot be 'pushed' in between the talc sheets. Once the pyroxene chains have been disconnected by loss of Ca they are comparatively free to move in the {010} plane. Breakdown of magnesic octahedra and subsequent loss of magnesium, silicon, and oxygen permits adjacent ferric-octahedral-tetrahedral chain segments

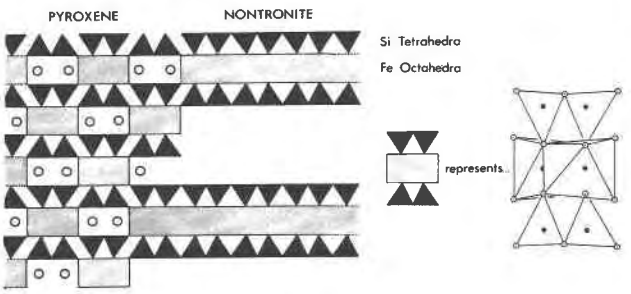

FIG. 5. Diagram of the relation between pyroxene and nontronite, viewed along the chain axis (pyroxene *z*).

to move into registry and so form a 'talc' sheet. One and a half cells of pyroxene have the same volume as one cell of nontronite, so that at constant volume:

$$1.5Ca_4Mg_{1.5}Fe_{2.5}Si_8O_{24} + 6\,H_2O \rightarrow Ca_{0.25}Mg_{0.5}Fe_{3.5}^{3+}Si_8O_{20}(OH)_4 4H_2O + Mg_{1.75}Fe_{0.25}Si_4O_{12} + Ca_{5.75} + O_2$$

which is very close to the production of nontronite by loss of Ca and the Mg octahedra with their flanking Si tetrahedra.

Figure 5 shows a diagrammatic representation of the relation between the two structures. The boundary between pyroxene and nontronite domains is coherent, and similar to a crystallographic shear plane. A relative shift of ½[10$\bar{1}$] between adjacent pyroxene chains produces the nontronite 'talc' sheet (Fig. 6).

Discussion

Loughnan (1969) describes silicate weathering as involving three simultaneous processes: the

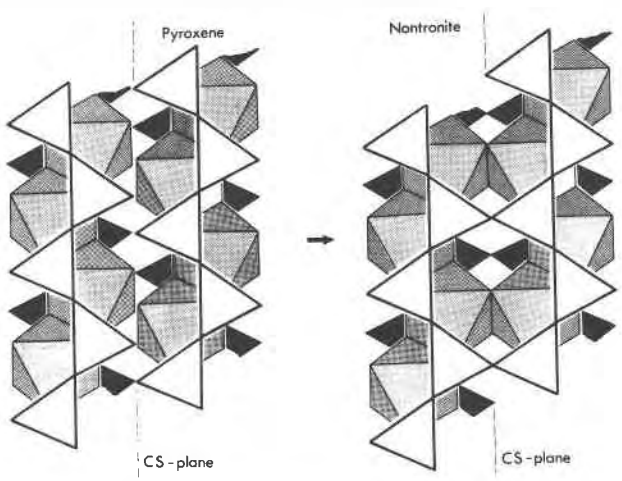

FIG. 6. View of pyroxene and nontronite normal to the cleavage. ({100} cpx, {001} non). CS – crystallographic shear.

breakdown of the parent structure with release of cations, the removal of released cations, and the addition of atmospheric components to form new minerals. These processes are all confirmed for the conversion of pyroxene to nontronite, but the breakdown of the parent structure is minimal, or as Loughnan writes (p. 31) "... much of the parent mineral structure is inherited by the secondary products."

Fieldes and Swindale (1954) concluded that layer silicate clay minerals form as residues from micas, but that "the structures of all other primary silicates are such that they cannot form layer silicates without first passing through an amorphous stage." This is clearly not the case in the formation of nontronite from pyroxene, and probably not for other transformations. In extending the model described here, it is significant that initial alteration occurs as the development of domains well ahead of the alteration 'front,' and that the alteration product has the same cell dimensions as the parent mineral. The degree of misfit controls maximum domain size, so that, for example, a pyroxene of different composition might be disrupted by development of nontronite domains greater than a few unit cells wide because of the strain at domain boundaries. The resulting body of clay might be pseudomorphous after pyroxene, but would not be obviously topotaxial.

Considerations such as these may also bear on the general problem of mineral stability during weathering. Other things being equal (for example, chemistry as in kyanite and andalusite or structure as in actinolite and hornblende), the mineral whose weathering product best fits the parent lattice may persist longer during weathering. Growth of ill-fitting domains ruptures (or collapses) the parent structure, allowing readier penetration of air and water and so hastens weathering.

Conclusion

Weathering of magnesium-rich hedenbergite removes all the Ca, most of the Mg, and some Si, oxidizes the iron, and allows the Si–Fe tetrahedral-octahedral chains to move in {010}. Coalescence of chains forms a dioctahedral ferric iron 'talc' layer in crystallographic continuity with the parent pyroxene. Nucleation of the nontronite is homogeneous over areas at least 2μ on a side and probably larger. Over any pyroxene crystal, the newly-formed nontronite domains all have the same orientation inherited from the pyroxene, so that when the pyroxene is gone, a single crystal of nontronite remains.

Acknowledgments

Most of this work was done while I was on leave at the Geology Department of the University, Manchester. I am grateful to Professor J. Zussman and the staff at Manchester for use of equipment, and to Dr. P. Champness for access to, and advice on, using the electron microscope. Discussion with Dr. J. N. Boland clarified aspects of the transmission electron-microscopy. Mr. G. M. Taylor first drew attention to the clay outcrop, and I am grateful for his stimulus and interest in this project. Analyses for FeO and H_2O were made at the Australian Atomic Energy Commission and the U.S. Geological Survey at Menlo Park, California, respectively, through the courtesy of Dr. M. Florence and Dr. P. Bateman.

References

FIELDES, M., AND L. D. SWINDALE (1954) Chemical weathering of silicates in soil formation. *J. Sci. Tech. New Zealand,* **56,** 140–154.

GUINIER, A. (1963) *X-Ray Diffraction.* W. H. Freeman and Co., San Francisco and London.

LOUGHNAN, F. C. (1969) *Chemical Weathering of the Silicate Minerals.* New York, American Elsevier.

ROSS, C. S., AND S. B. HENDRICKS (1945) Minerals of the montmorillonite group. *U.S. Geol. Surv. Prof. Pap.* **205-B,** 79 pp.

Manuscript received, December 30, 1974; accepted for publication, July 10, 1975.